Int. J. Multiphase Flow, Vol. 7, pp. 211–219, 1981
Printed in Great Britain

0301-9322/81/020211-09$02.00/0
Pergamon/Elsevier

TWO-PHASE TWO-COMPONENT INTERFACE DRAG COEFFICIENTS IN SEPARATED PHASE FLOWS

W. R. MARTINDALE
Department of Mechanical Engineering, Montana State University, Bozeman, MT 59715, U.S.A.

and

R. V. SMITH
Department of Mechanical Engineering, Wichita State University, Wichita, Kansas, U.S.A.

(*Received* 12 *March* 1979; *in revised form* 27 *April* 1980)

Abstract—This work examines the behavior of the interface friction factor or drag coefficient as a means for extending the modeling of separated two-phase flows through the separate consideration of each phase. The model development of this work builds primarily upon the work of Carofano & McManus (1969), Wallis (1970) and Smith (1968). A one-dimensional flow model was developed for the case of vertical upward annular flow of an air–water mixture with droplet entrainment. The model was developed for the investigation of accelerating flows in a nozzle but is utilized in this study for the investigation of momentum transport occurring in non-accelerating flows. This study presents experimental data showing the behaviour of the flow pressure drop occurring at various flow qualities and gas velocities. Also presented are empirical results for values of the air–water interface drag coefficient as a function of flow quality and gas core Reynolds number. The drag coefficient variation is compared to a previous correlation developed by Wallis (1969).

INTRODUCTION

Experimental techniques to measure the actual drag occurring on an interface between two fluids are not available, hence, assumptions based upon fluid–solid measurements have normally been utilized. Fluid–solid measurements refer to measurements of drag in a fluid flow over a solid surface. The extrapolation of fluid–solid drag data would be valid if the fluid–fluid interface were rigid, but this is not the case. The gas–liquid interface for annular flows takes on a very wavy appearance which is primarily dependent upon the gas velocity and the liquid film thickness. An improvement in the information on interface drag coefficients has been achieved in this study.

This work examines the behavior of the interface friction factor or drag coefficient as a means for extending the modeling of separated two-phase flows through the separate consideration of each phase. The model development in this study is based primarily upon the work of Carofano & McManus (1969), Wallis (1970) and Smith (1968) in which momentum and energy transport equations are considered for each phase. A one-dimensional flow model was developed for the case of vertical upward annular flow of an air–water mixture with droplet entrainment. This model was developed for the investigation of the momentum transport occurring in non-accelerating flows of which this study is concerned.

ANALYSIS

A one-dimensional flow model was developed for vertical upward annular flows of air and water with droplet entrainment. The model equations were written for the case of a general axi-symmetric duct geometry but this paper investigates only the case of a constant diameter circular duct. Figure 1 shows a differential element of the flow model. Although only the constant flow area case is considered in this paper, the analysis is developed for the more general case of variable flow area. The gas–liquid interface was assumed to possess a smooth, unrippled surface with the liquid film uniformly distributed around the periphery of a cross section. The liquid film terms will, however, incorporate an empirical correction for surface waves and flow blockage. The gas–core flow was assumed to be turbulent in nature

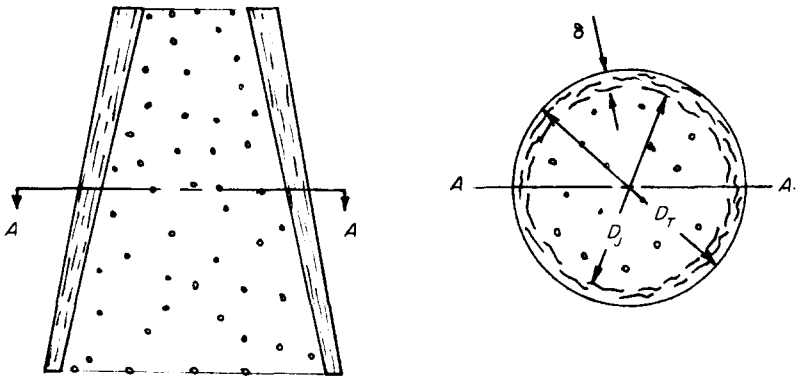

Figure 1. Flow model element.

with a uniform dispersion of spherical droplets of a uniform size carried within the gas-core flow.

The distinct regions of the flow were considered and momentum and mass conservation equations were written for each region. The momentum equation written for the gas core yields the following equation for the pressure gradient along the duct. The first two terms in the numerator are the drag forces resulting from the air–water interface and the entrained droplets respectively. The third term in the numerator is the momentum force which equals zero in this study.

$$\frac{dP}{dl} = \frac{-C_{D_i}\frac{\rho_G}{2}(V_G - V_L)^2\pi D_G - C_{D_d}\frac{\rho_G}{2}(V_G - V_d)^2 A_d - \dot{m}_G\frac{dV_G}{dl}}{A_G} \qquad [1]$$

where P is pressure, L is the axial length along the flow duct, C_{D_i} is the coefficient of gas–liquid film interface drag, ρ_G is the gas density, V_G is the gas velocity, V_L is the liquid velocity, D_G is the gas flow diameter, C_{D_d} is the coefficient of droplet drag, A_G is the cross-sectional area of the droplet and $\dot{m}_G$ is the mass flow rate of the gas.

Writing the continuity equation for the gas core yields the expression for the gas velocity gradient.

$$\frac{dV_G}{Dl} = -\dot{m}_G\left(\frac{1}{\rho_G A_G^2}\frac{dA_G}{dl} + \frac{1}{\rho_G^2 A_G}\frac{d\rho_G}{dl}\right). \qquad [2]$$

In a similar manner for the liquid film from the momentum equation, the liquid velocity gradient is given as:

$$\frac{dV_L}{dl} = \frac{C_{D_i}\frac{\rho_G}{2}(V_G - V_L)^2\pi D_G - C_{D_w}\frac{\rho_L}{2}V_L^2\pi D_T - \rho_L g A_L - A_L\frac{dP}{dl}}{\dot{m}_L} \qquad [3]$$

where C_{D_w} is the coefficient of duct wall drag, D_T is the total duct diameter, A_L is the liquid flow area, and $\dot{m}_L$ is the mass rate of flow of the liquid.

The first two terms in the numerator are the drag forces arising from the air–water interface and the wall friction respectively. The third term in the numerator is the pressure force. This equation is identically zero for this study. The droplet velocity gradient was obtained by applying Newton's law to a single droplet as given in [4].

$$\frac{dV_d}{dl} = \frac{C_{D_d}\frac{\rho_G}{2}(V_G - V_d)^2 A_d}{m_d V_d} \qquad [4]$$

where A_d is the area of the droplet, and m_d is the mass of the droplet. Invoking continuity for the liquid film and an expression for the duct area in terms of the gas and liquid area yields

$$\frac{dA_G}{dl} = \frac{dA_T}{dl} + \frac{\dot{m}_L}{\rho_L V_L^2}\frac{dV_L}{dl}. \quad [5]$$

For the constant area duct of this study $dA_T/dl = 0$. This expression for the gas area axial variation assumes that the entrained droplets area does not change within the length of the element size (allowance is made for the droplets to change size discontinuously during numerical integration, however). The criteria used to establish a change in the droplet area was that used by Rabin *et al.* (1960) which allows a droplet to break up or shatter once the shear stress forces on the droplets exceed the surface tension forces. Droplet breakup was considered to occur when the following expression was satisfied.

$$\frac{We}{(Re)^{0.5}} = \frac{\rho_L (V_G - V_d)^2 \frac{D_d}{\sigma}}{\left((V_G - V_d)\frac{D_d}{\nu_G}\right)^{0.5}} > 1.0 \quad [6]$$

where We is the Weber number, Re is the Reynolds number, σ is the surface tension and ν_G is the dynamic viscosity of the gas.

Assuming these conditions [6] no breakup was found to occur in the experimental conditions of this study. Droplet shatter is predicted by [6] in extrapolations shown in figure 5. This is known to produce many smaller size droplets, although much information on this droplet size distribution is lacking. This study assumes that once droplet shatter occurs, the original droplet diameter will be reduced to one-third the initial value while maintaining a constant entrainment fraction. For the duct geometry of this study, droplet breakup is not a major concern. Investigations by Smith (1968) have indicated that variations in effective droplet diameter do not result in significant variations in the pressure profile.

Conservation of energy was considered for the gas core, the liquid film, and the entrained droplets. Droplets are actually being continuously entrained in the gas flow and redeposited in the liquid film, although the droplets travel in the gas stream for some distance before being redeposited. The residence time for these droplets in the gas core is not known, but would depend upon the droplet size, the gas velocity, and the gas flow cross-sectional area. Considering this interchange of liquid between the film and gas core, the droplet temperature was assumed to remain the same as the liquid film at a given cross section. The entire analysis assumes isothermal flow. This assumption was partially verified through the energy equations solved in a parallel study (Martindale & Smith 1981). The ideal gas equation in differential form relates the air density gradient.

$$\frac{d\rho_G}{dl} = \frac{1}{RT_G}\frac{dP}{dl} - \frac{P}{RT_G^2}\frac{dT_G}{dl} \quad [7]$$

where R is the gas constant, T_G is the gas temperature, and $dT_G/dl = 0$.

Expressions for the shearing stresses and drag production were written in terms of friction factors or drag coefficients. The drag produced by the entrained droplets was accounted for through an expression used by Carofano & McManus (1969) which correlated droplet drag coefficient values for falling droplets which undergo a distortion of shape.

$$C_{D_d} = 0.271\,(Re_d)^{0.217}, \quad 400 \le Re_d \le 10{,}000 \quad [8]$$

where Re_d is the Reynolds number for the droplet.

The solid wall–liquid film friction factor or drag coefficient was set to a constant value of 0.0015. This value is one third of the value normally cited in the literature for the Fanning friction factor. An analysis of the wall shear stress for an annular flow, based upon laminar boundary layer theory and a rigid gas–liquid interface, produced wall friction factor values only slightly above 0.0015. The duct walls were an extruded polyvinyl with a highly smooth surface so their roughness would not be a significant factor.

An adequate description of the entrained droplet diameter as a function of the flow conditions was not available. The work of Smith (1968) and that of Carofano & McManus (1969) determined that an effective droplet diameter could be characterized as

$$D_d = 0.122 \text{ mm}.$$

This value was utilized in this analysis. The entrained droplets were characterized as uniformly distributed, with a given number of droplets contained in a cross-sectional plane and the number of these planes uniformly spaced (see figure 2). Values assigned for the number of droplet planes and the number of drops per plane were determined from the entrainment data of Wallis (1966) for each set of flow conditions.

In this study the term dS_L/dl, where S_L is the surface area of the liquid, was evaluated for a uniform, flat interface. The actual irregular nature of the gas–liquid interface created areas where a form drag may arise. The regions can also exist downstream of the entrained droplets. Because these regions create a blockage to the gas flow they were accounted for by the use of a blockage factor applied to the calculations of the pressure gradient and gas velocity, where a gas area correction was needed. The application of the blockage factor was applied to these terms only so that the liquid area is not actually changed from the smooth surface assumptions. The gas corrected area term was employed in the form

$$A'_G = A_G(1 + BF) = A_T(BF) \qquad [9]$$

where A'_g is the corrected cross-sectional area of the gas flow, and BF represents a blockage factor included to indicate the droplet wakes and film wave troughs which are volumes prohibited for use of high velocity gas flow. Values of the blockage factor used in this work were taken from the photographic work of Lindsted (1977) which was based upon the same flow duct geometry used in this study. Lindsted correlated a blockage factor of the form

$$BF = \frac{A_T - A_\delta - A_d - A_{\text{wave}}}{A_T - A_\delta} \qquad [10]$$

(where A_δ is the area of the liquid film) to the flow conditions for upward-annular flows of air and water. The subscripts in the equation above refer to cross-sectional areas where T is the total duct area, δ is the mean film area (excluding wave crests), d is the droplet area and A_{wave} is the area of the wave crests. The numerical values of the blockage factor used did not vary significantly. They ranged in value from 0.88 to 1.0 throughout the entire range of flow conditions of this study. The lower values occurred for those conditions of low flow quality and low gas velocity.

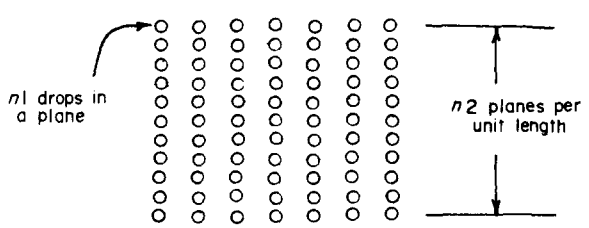

Figure 2. Entrained flow element.

The model equations were solved numerically using a Runge–Kutta scheme and input flow conditions matching the experimental data. The integration was carried out over a 200 cm length of the duct and the value of the air–water interface drag coefficient was varied until the integration produced the experimental values of the pressure drop over that distance. Initial values of the liquid film velocity were varied along with the interface drag coefficient until a stable and essentially constant liquid velocity was achieved and the gas velocity and pressure drop matched the experimental measurements. Further details of the model development and integration can be found in Martindale (1977).

EXPERIMENTAL

The experimental system used in the constant duct diameter flow tests is shown in figure 3. The vertical section of the system consisted of a 312 cm long, 32 mm i.d. transparent acrylic tube. Water was injected through the tube walls into the air stream at the bottom of the vertical section. The air–water mixture traveled upward through the vertical section, in which pressure taps were mounted, and the mixture was exhausted to the atmosphere. Air flow rate measurements were made using a concentric orifice designed to ASME specifications. Air temperature was controlled by initially passing the air through a heat exchanger immersed in the water reservoir so the mixing air and water were then initially at the same temperature. Water flow rate measurements were obtained by a timed weighing at the system exhaust. Two static pressure taps were installed in the duct walls and spaced 200 cm apart. The taps fed directly into a liquid trap and then to a water-filled manometer to measure the pessure drop. System pressure was obtained at the location of the upstream pressure tap from a bourdon tube gauge and barometer reading.

The complete pressure drop data from the experimental program are shown in figure 4. Superficial gas velocities were used in the reduction of the data. The data, which is plotted non-dimensionally as the ratio of two-phase drop in pressure to the gas only (superficial velocity) drop in pressure, show a surprising behavior of this ratio with respect to gas velocity.

One would expect that for a constant quality an increase in the gas velocity (gas mass flow rate increase) would produce a higher ratio of two-phase to gas only drop in pressure, but the opposite is seen to occur. The authors believe that the most likely explanation is the effect of liquid–gas interfacial waves and particularly of the formation of large disturbance waves which

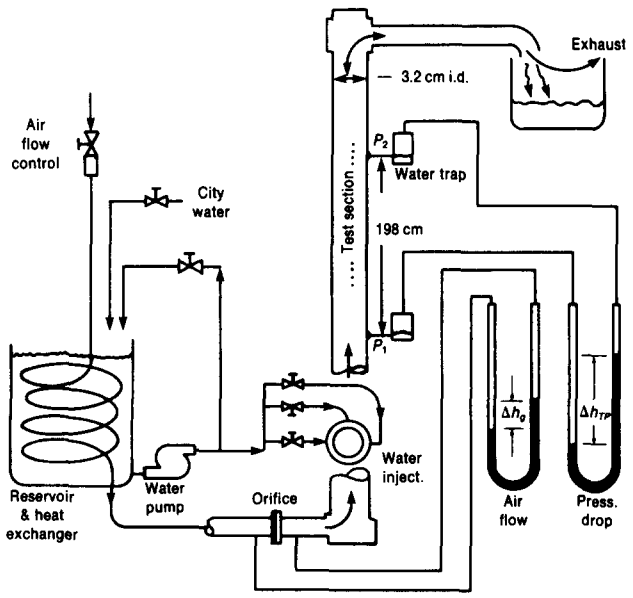

Figure 3. Experimental system.

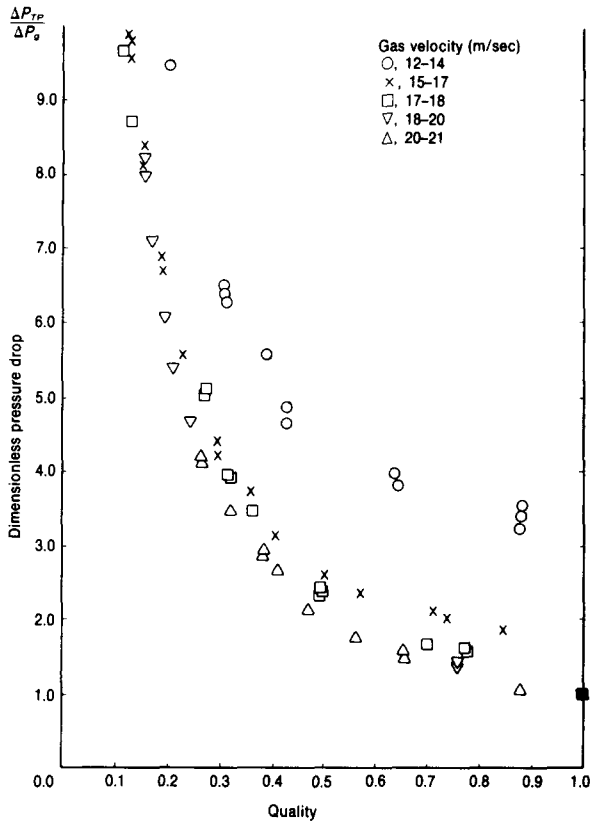

Figure 4. Dimensionless pressure drop variation.

are on the annular liquid film next to the wall and travel at a velocity substantially higher than the mean velocity of the liquid in the wall film. Somewhat similar findings of pressure drop behavior have been reported by Carofano & McManus (1969), Chien & Ibele (1964) and Hewitt & Hall-Taylor (1970). Further discussion of the pressure drop behavior can be found in Martindale & Smith (1981).

The method used in producing a useful working drag coefficient was to incorporate all the terms which are analytically and experimentally difficult to assess. This would include terms such as the momentum transport arising from droplet entrainment and redeposition.

The empirically derived interface drag coefficients are shown in figure 5. The curves shown were extrapolated beyond a gas core Reynolds number of approx. 100,000 for use in studies involving a variable duct geometry. The portion of the curves to the left of the indicated upper limit was constructed from the experimental data of this study. These coefficients are plotted as a function of the gas-core Reynolds number for constant quality flows. The variation of these coefficients is seen to fall rapidly with increasing Reynolds number up to a Reynolds number of 10^5 beyond which the drag coefficients tend to level out. The curves fall below both the empirical values for gas only flow (100 per cent quality) and the Fanning turbulent correlation for smooth pipes. The 100 per cent quality line was calculated by setting the liquid flow rate equal to a very small number and entrainment equal to zero in the governing equations. This was done to avoid a discontinuity which occurred for zero liquid flow rate. The experimental values of gas only pressure drop were used in obtaining the interface drag coefficient variation. The reason for the behavior of the drag coefficient values falling below the Fanning turbulent correlation is not understood. This could possibly be the result of droplets in the gas core smoothing the turbulence intensity of the gas core. A possible analogy of this behavior has been well demonstrated with the use of wire mesh screens in wind tunnels. This action by droplets would tend to give drag coefficient values more in line with a laminar type gas flow as they

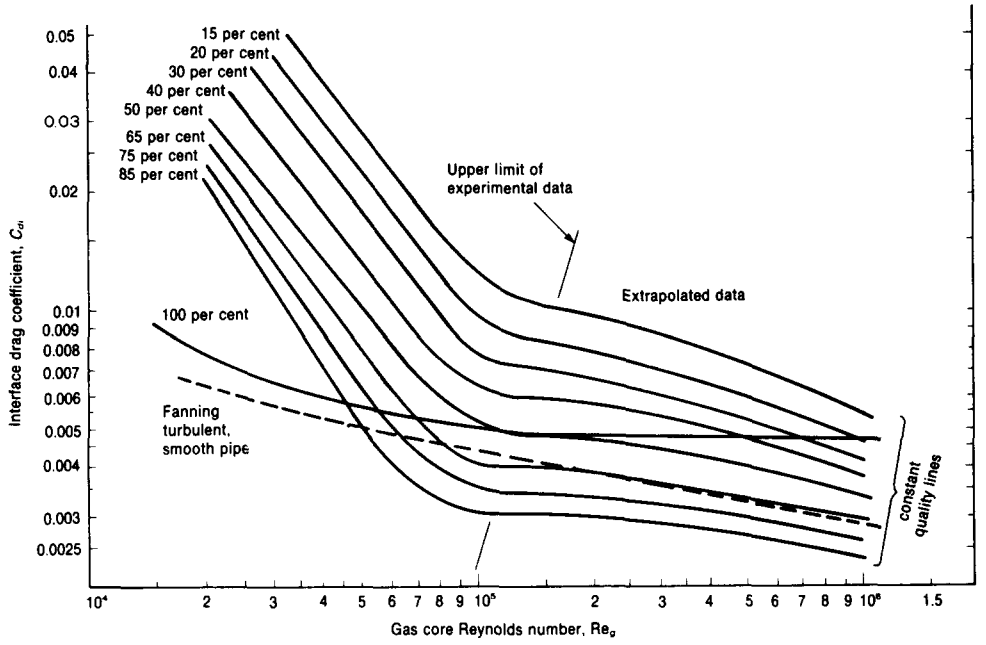

Figure 5. Constant area model prediction of interface drag coefficient.

show. This behavior might also be rationalized by an excessive pressure drop shown by the analysis as a contribution of the entrained flow drag coefficients. This would produce a reduced pressure drop as a result of the interface momentum transport and would be reflected in the derived drag coefficient values. It is seen that the model equations and the evaluative procedure produce reasonable agreement with the gas only flows and the Fanning smooth pipe turbulent flow correlation.

The more steeply inclined slope of the interface drag coefficient at Reynolds numbers below 10^5 is suggestive of the effects of waves occurring on the interface. The highly wavy nature of the interface is visible in this range of Reynolds numbers and appears more suppressed or flattened in the higher Reynolds number range.

The drag coefficient variation with quality shows a dependence upon the thickness of the annular film. The empirical values of the drag coefficient as a function of the film thickness are shown in figure 6. The values of film thickness used in this case are also empirically derived and are not actual measurements. Figure 6 indicates a reasonable agreement with a correlation derived by Wallis (1969) showing a dependence solely upon the dimensionless film thickness. The data scatter in this plot is too large to relate an extensive comparison to the corelation of Wallis, but the mean value line shown plotted does show some similarity to that due to Wallis.

CONCLUSIONS

A one-dimensional model was developed for a general axisymmetric two-phase, two-component upward annular flow. The interface drag coefficient values derived from the model show that the nature of the interface plays an important role in the drag on the gas core as does the flow quality and the gas Reynolds number. The drag coefficient variation indicates a critical value of the gas core Reynolds number above which the wavy nature of the interface becomes less pronounced and the drag coefficient becomes less sensitive to changes in the gas core Reynolds number for a particular flow quality. The results produced by this investigation have raised some interesting questions which will require further investigation. The gas core flow can reasonably be expected to be turbulent in nature but the drag coefficient behavior shows, for lower quality flows, that the turbulence may be attenuated significantly. The role of the

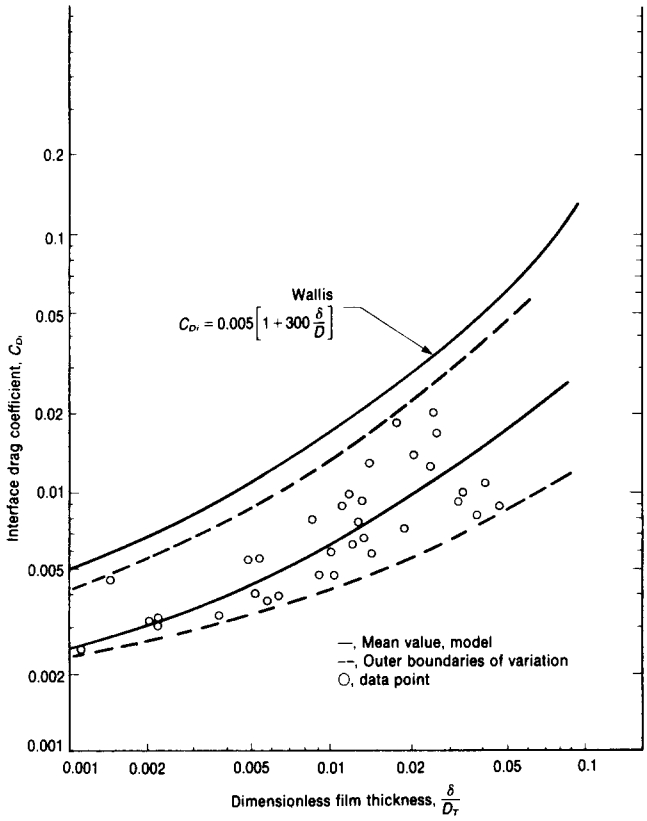

Figure 6. Correlation of interface drag coefficient to dimensionless film thickness.

entrained droplets in producing this effect has been investigated, but further work is needed to give a better understanding of the behavior of the gas flow during these types of two-phase flows.

Acknowledgements—The authors would like to acknowledge the support from the National Science Foundation Grant GK38425 which was active in the first portion of this study. The authors would also like to acknowledge the assistance of Dr. R. D. Lindsted whose counsel and data were extremely valuable to the results shown herein.

REFERENCES

ANDERSON, G. H. & MANTZOURANIS, G. B. 1960 Two-phase (gas–liquid) flow phenomena—I. *J. Chem. Engng Sci.* **12**, 109–126.

BROWN, D. J., JENSEN, A. & WHALLEY, P. B. 1975 Non-equilibrium effects in heated and unheated annular two-phase flow. ASME Paper 75-WA/HT-7.

CAROFANO, G. C. & MCMANUS, JR., H. N. 1969 An analytical and experimental study of the flow of air–water and steam–water mixtures in a converging–diverging nozzle. *Prog. Heat and Mass Transfer* **2**, 395–417.

CHIEN, S. & IBELE, W. 1964 Pressure drop and liquid film thickness of two-phase annular and annular mist flows. *J. Heat Transfer* **83**, 89–96.

HEWITT, G. F. & HALL-TAYLOR, H. 1970 *Annular Two-Phase Flow.* Pergamon Press, Oxford.

LINDSTED, R. D. 1977 A photographic technique to obtain droplet and flow pattern data in two-phase flow for use in modeling. Ph.D. Thesis, University of Oklahoma.

MARTINDALE, W. R. & SMITH, R. V. 1981 Two-phase nozzle flow. *Int. J. Multiphase Flow.* Submitted.

MARTINDALE, W. R. 1977 Two-phase air–water upward annular flow in a converging nozzle. Ph.D. Thesis, Wichita State University, Wichita, KS.

MARTINDALE, W. R. & SMITH, R. V. 1980 Pressure drop and sonic velocity in separated two-phase flows. *Trans. ASME J. Fluids Engng* **102**, 112–114.

RABIN, E., SCHALLENMULLER, A. R. & LOWHEAD, R. B. 1960 Displacement and shattering of propellant droplets. Final Summary Rep. AFOSR TR 60-75, Rocketdyne, Division of North American Aviation, Inc., March.

SMITH, R. V. 1968 Two-phase, two-component, critical flow in a venturi. Ph.D. Thesis, University of Oxford.

WALLIS, G. B. 1969 *One-Dimensional Two-Phase Flow*, pp. 318, 323. McGraw-Hill, New York.

WALLIS, G. B. 1966 AEC Rep. NYO-3114-14, EURAEC 1605.

WALLIS, G. B. 1969 Papers 69-FE-45, ASME Applied Mech. Fluids Engng Conf., Northwestern University, June.

WALLIS, G. B. 1970 Annular two-phase flow. *Trans. ASME, J. Basic Engng* **92–93**, 59–82.

WARNER, C. F. & NETZER, D. W. 1963 An investigation of the flow characteristics of two-phase flow in converging–diverging nozzles. ASME Paper 63-WA-192.